A specific monovalent metal ion integral to the AA platform of the RNA tetraloop receptor

Soumitra Basu[1], Robert P. Rambo[2,3], Juliane Strauss-Soukup[1], Jamie H. Cate[2,4], Adrian R. Ferré-D´Amaré[2], Scott A. Strobel[1] and Jennifer A. Doudna[2,3]

Metal ions are essential for the folding and activity of large catalytic RNAs. While divalent metal ions have been directly implicated in RNA tertiary structure formation, the role of monovalent ions has been largely unexplored. Here we report the first specific monovalent metal ion binding site within a catalytic RNA. As seen crystallographically, a potassium ion is coordinated immediately below AA platforms of the *Tetrahymena* ribozyme P4-P6 domain, including that within the tetraloop receptor. Interference and kinetic experiments demonstrate that potassium ion binding within the tetraloop receptor stabilizes the folding of the P4-P6 domain and enhances the activity of the *Azoarcus* group I intron. Since a monovalent ion binding site is integral to the tetraloop receptor, a tertiary structural motif that occurs frequently in RNA, monovalent metal ions are likely to participate in the folding and activity of a wide diversity of RNAs.

Metal ions act as essential cofactors in the folding of large catalytic RNAs. The identification of metal ion binding sites within RNA has focused almost exclusively on divalent ions, such as Mg^{2+}, which play both a structural and a catalytic role in many ribozymes[1]. Despite this emphasis on divalent ions, many catalytic RNAs explicitly require monovalent ions such as potassium or ammonium to achieve catalysis *in vitro*[2,3], and the ribosome requires monovalent ions to function *in vitro*[4,5]. These ions are thought to provide nonspecific charge neutralization of the phosphate backbone requisite to globular RNA folding[6]. The possibility of specific and functional monovalent metal ion binding sites within RNA has been largely unexplored.

The tertiary interaction between a GAAA tetraloop and an 11-nucleotide tetraloop receptor is a common structural motif for RNA folding (Fig. 1*a*). The tetraloop receptor is a highly conserved and modular motif present in a wide variety of RNAs including group I and II introns, and RNaseP[7]. This structural element includes two consecutive As that are aligned side-by-side to form a pseudo base pair, termed an AA platform (underlined bases in Fig. 1*a*), which stacks with the As in the GAAA tetraloop[8,9]. Immediately below the AA platform is a non-canonical base pair (either a G·U wobble pair or a non-Watson-Crick A·U pair) that is also a conserved part of the motif[9].

There are three AA platforms in the P4-P6 domain of the *Tetrahymena* group I intron, and all three mediate long-range RNA tertiary interactions (Fig. 1*b*)[9]. Two of the platforms (L5c and J6/6a) participate in intermolecular contacts between adjacent P4-P6 molecules in the crystal, while the J6a/6b platform forms part of the tetraloop receptor and makes intramolecular contact with the L5b tetraloop. Mutagenesis experiments have demonstrated that the interaction between the L5b tetraloop and the J6a/6b tetraloop receptor is essential for folding of the domain[9,10].

The AA platforms in J6/6a and J6a/6b are both adjacent to a G·U wobble pair. Within the P4-P6 crystal structure, there are peaks of electron density between the planes of the pseudo A·A pair and the wobble pair (Fig. 1*c*)[9]. Soaking the P4-P6 RNA crystals with Mn^{2+} did not result in peaks at these positions in an anomalous difference Fourier electron density map[11], nor did they correspond to sites of metal hexammine binding[12]. These observations suggest that the residual electron density in the major groove above the wobble pair may be due to water or K^+, which is the only other metal cation present in the P4-P6 crystallization solution[8].

Monovalent ion binding sites

To test the identity of the unexplained electron density below the AA platforms, P4-P6 crystals were soaked in solutions containing Tl^+ or Cs^+. These ions have strong anomalous diffraction signals and ionic radii comparable to K^+ (K^+, 1.33 Å; Tl^+, 1.40 Å; and Cs^+ 1.69 Å)[13]. X-ray diffraction intensities measured from these crystals were used to calculate anomalous difference Fourier electron density maps. Strikingly, Tl^+ produced a map containing just three peaks greater than 7.5σ in size. Two of these peaks occur directly under the J6a/6b and J6/6a platforms (13.5 and 10σ respectively) (Fig. 2*a*). The third peak is close to, but not directly under the L5c AA platform (11σ). These binding sites show some preference for the size of the metal ion, since cesium, which has a larger ionic radius than thallium, produced sites of lesser intensity (the J6a/6b peak is 7σ, J6/6a is 6σ, and L5c is 10σ).

The thallium ion binding sites under the J6/6a and J6a/6b platforms are identical. Each site appears to involve five direct coordinations to the RNA, including the 2'-OH of the first (5') A in the platform, the pro-R_P phosphate oxygen between the As of the platform, the O6 and N7 groups of the G immediately below the platform, and the O4 of the U two bases below the pseudo pair (Fig. 2*b*). The monovalent ion does not participate directly in interdomain tertiary interactions, but instead appears to organize the AA platform for participation in such contacts.

The AA platform in L5c is adjacent to a non-canonical A·U, rather than a G·U pair. This platform appears to be supported by a magnesium ion, which coordinates to the pro-R_P phosphate oxygen between the AA pseudo pairs. The Tl^+ binds adjacent to the L5c

[1]Center for Chemical Biology, [2]Center for Structural Biology, [3]Howard Hughes Medical Institute, Department of Molecular Biophysics and Biochemistry, Yale University, New Haven, Connecticut, 06520, USA. [4]Present Address: University of California, Santa Cruz, California 95064, USA.

Correspondence should be addressed to S.A.S. *email: strobel@csb.yale.edu* or J.A.D. *email: doudna@csb.yale.edu*

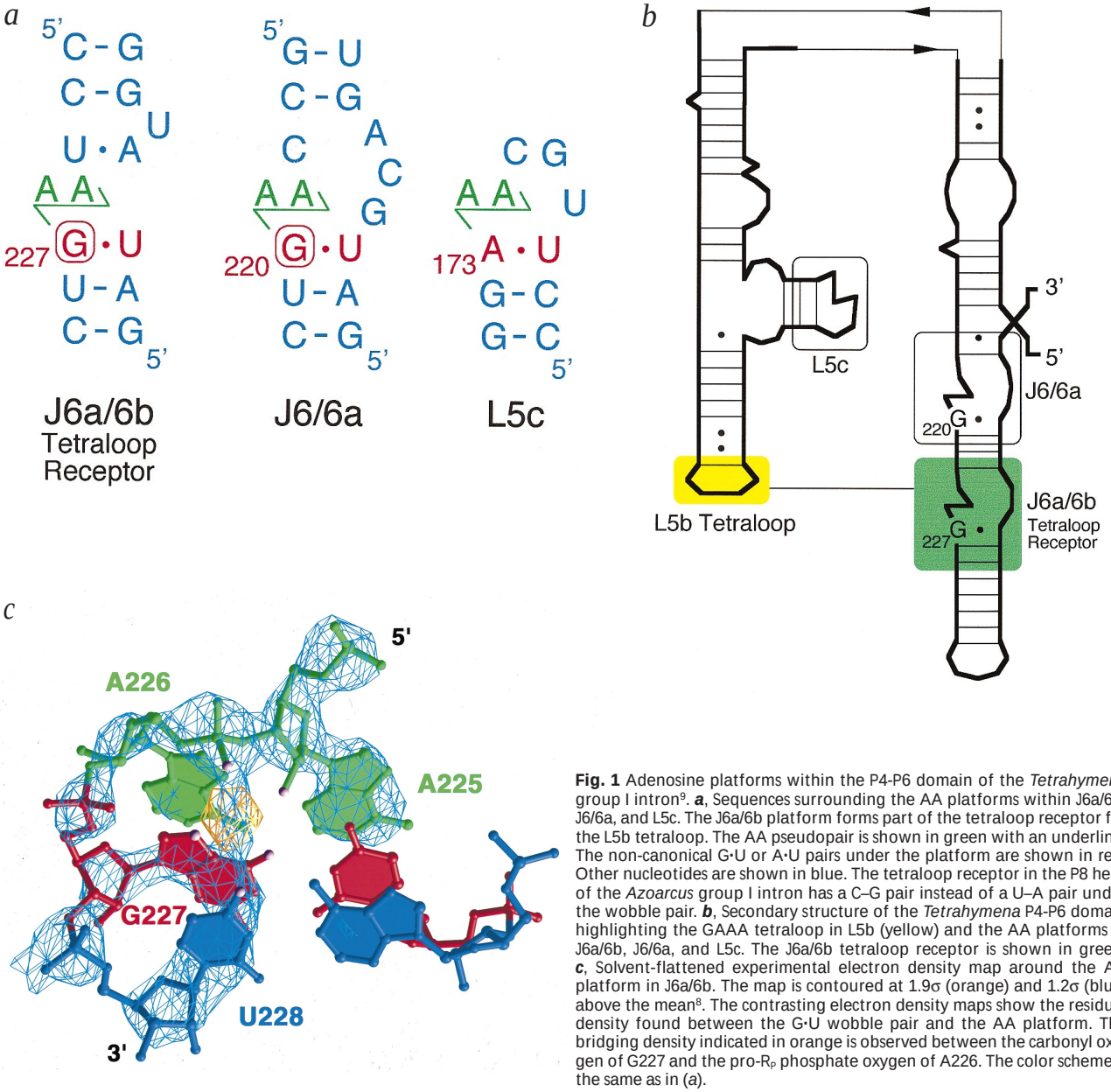

Fig. 1 Adenosine platforms within the P4-P6 domain of the *Tetrahymena* group I intron[9]. ***a***, Sequences surrounding the AA platforms within J6a/6b, J6/6a, and L5c. The J6a/6b platform forms part of the tetraloop receptor for the L5b tetraloop. The AA pseudopair is shown in green with an underline. The non-canonical G·U or A·U pairs under the platform are shown in red. Other nucleotides are shown in blue. The tetraloop receptor in the P8 helix of the *Azoarcus* group I intron has a C–G pair instead of a U–A pair under the wobble pair. ***b***, Secondary structure of the *Tetrahymena* P4-P6 domain highlighting the GAAA tetraloop in L5b (yellow) and the AA platforms in J6a/6b, J6/6a, and L5c. The J6a/6b tetraloop receptor is shown in green. ***c***, Solvent-flattened experimental electron density map around the AA platform in J6a/6b. The map is contoured at 1.9σ (orange) and 1.2σ (blue) above the mean[8]. The contrasting electron density maps show the residual density found between the G·U wobble pair and the AA platform. The bridging density indicated in orange is observed between the carbonyl oxygen of G227 and the pro-R_P phosphate oxygen of A226. The color scheme is the same as in (*a*).

AA platform at a site that also binds metal hexammines and hydrated magnesium ion[11,12]. Thus, the Tl^+ appears to be binding to a general metal ion site.

Nucleotide analog interference mapping

The crystallographic results suggested that specific monovalent ion binding sites may stabilize the folding of the P4-P6 domain. To explore the functional importance of specific monovalent ion binding sites within the P4-P6 domain, we employed nucleotide analog interference mapping (NAIM)[14,15]. We synthesized 5'-*O*-(1-thio)-6-thioguanosine triphosphate ($S^6G\alpha S$) (Fig. 3*a*) and randomly incorporated it into the P4-P6 domain at a level of less than one substitution per molecule to test for metal coordination to the O6 carbonyl oxygen of G in the major groove, one of the RNA functional groups implicated in direct monovalent metal ion coordination. $S^6G\alpha S$ has two important features essential for its use in NAIM: (i) it substitutes the hard Lewis base O6 of G with a soft Lewis base sulfur, which may interfere with alkaline metal ion binding[16,17]; and (ii) it has an α-phosphorothioate substitution that makes it possible to identify the sites of 6-thioguanosine incorporation by cleavage of the phosphate linkage with iodine[18]. We separated folded variants of the P4-P6 domain from the unfolded RNAs by native gel electrophoresis[10] and characterized the distribution of $S^6G\alpha S$ cleavage products within these populations to determine the importance of the O6 carbonyl at each position in the transcript.

In the folded P4-P6 fraction there was strong (>10 fold) $S^6G\alpha S$ interference at G227, the G located immediately below the AA platform in the J6a/6b tetraloop receptor (Fig. 3*b*, compare lanes 1 and 3 to lanes 4 and 6; Fig. 3*c*). The band intensities at G227 for GαS were equivalent between the folded and unselected fractions, which indicates that $S^6G\alpha S$ interference was not due to a phosphorothioate effect. Interference was not detected at any other positions within P4-P6, including the equivalent G adjacent

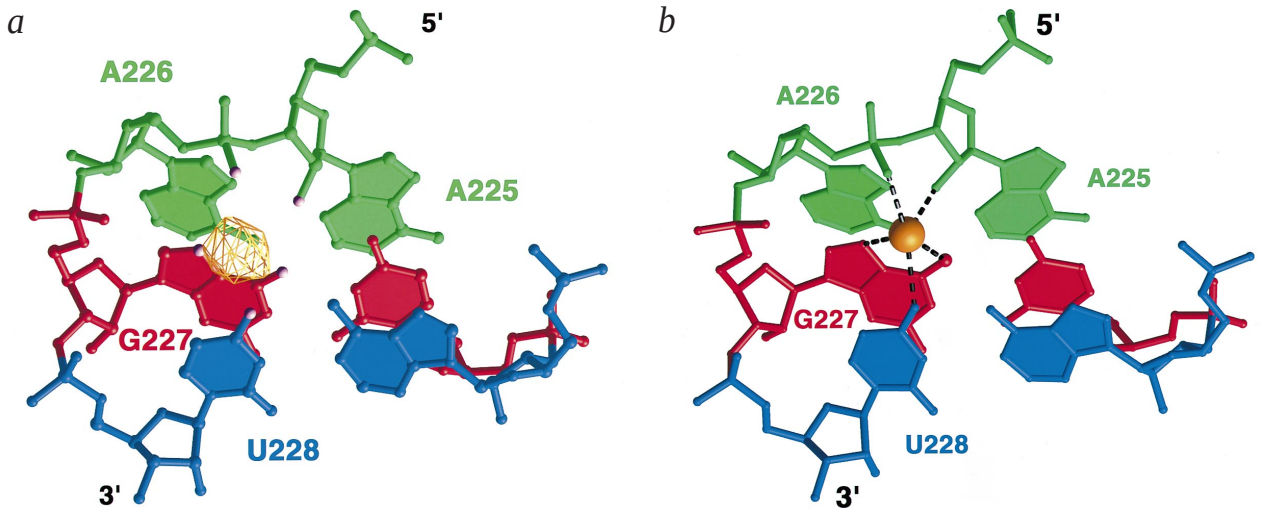

Fig. 2 Thallium binding sites in the P4-P6 domain. ***a***, Anomalous difference Fourier electron density map of J6a/6b. The electron density is contoured to 8σ above the mean. ***b***, Coordination of the monovalent cation within the binding pocket of the J6a/6b platform which acts as a tetraloop receptor. The metal ion is shown in orange and the metal-ligand interactions are shown in black. The color scheme is as described in Fig. 1. Both figures were prepared in RIBBONS[44].

to the J6/6a AA platform (G220). Lack of interference at G220 is consistent with the observation that the J6/6a platform does not contribute to an intramolecular tertiary contact within P4-P6[9].

Interference at G227 from $S^6G\alpha S$ may be due to disruption of a monovalent metal binding site within the tetraloop receptor or it may result from a steric destabilization of the AA platform caused by the larger atomic radius of the sulfur. To distinguish between these possibilities, we attempted to rescue $S^6G\alpha S$ interference at G227 by the addition of Tl^+. Tl^+ is an ideal candidate for interference rescue because it is a soft monovalent Lewis acid that may be able to coordinate the sulfur of $S^6G\alpha S$[16], it can form stable complexes with sulfur compounds such as thiourea[19], and it binds to the unmodified J6a/6b site in the crystal structure. We found that the inclusion of as little as 1 mM Tl^+ in the incubation and gel matrix buffers resulted in the complete rescue of $S^6G\alpha S$ interference at G227 (Fig. 3*b*, compare lanes 2 and 3 to lanes 5 and 6; Fig. 3*c*). Interference at G227 was not efficiently rescued by the soft divalent Lewis acid Mn^{2+} or by the addition of up to 100 mM of the hard monovalent Lewis acids K^+ or Rb^+, which have an ionic radius similar to that of Tl^+, but are not soft Lewis acids (data not shown). Furthermore, Tl^+ rescue of G227 $S^6G\alpha S$ interference was quite specific. Previously reported sites of $A\alpha S$ phosphorothioate interference (A139, A184, A186, and A187)[11] were unaffected by the addition of the monovalent metal (Fig. 3*c*). The pro-R_P oxygens of A184, A186, and A187 participate in Mg^{2+} binding[11], so lack of Tl^+ rescue at these sites is an important negative control for monovalent metal ion specific rescue. Only the $A\alpha S$ interference at A171 showed a slight rescue (~two-fold; Fig. 3*c*). Interestingly, A171 is one of the two As in the L5c AA platform, and its pro-R_P oxygen has been shown to make inner sphere coordination to a Mg^{2+} ion that supports this form of the AA platform motif. These interference data argue that P4-P6 domain folding is stabilized by coordination of a monovalent metal ion to the G227 carbonyl within the J6a/6b tetraloop receptor. We have demonstrated that this is a K^+ site in the P4-P6 crystal, but in the context of a 6-thioguanosine substitution at G227, Tl^+ appears to coordinate effectively.

We tested for interference at G220 and G227 in the context of the complete *Tetrahymena* intron using an exon ligation activity assay with the L-21 G414 RNA[15], but did not observe interference at these sites. This is consistent with previous interference experiments which showed that while the tetraloop–tetraloop receptor interaction is necessary for P4-P6 folding, it is not essential for *Tetrahymena* splicing activity[20].

Monovalent site important for intron splicing

If there is a general requirement for a monovalent metal ion within the tetraloop receptor, then there should be monovalent ion binding sites in other RNAs containing this folding motif. To address this possibility, we performed the $S^6G\alpha S$ interference experiments on the *Azoarcus* group I intron, which has a tetraloop–tetraloop receptor interaction between the P2 and P8 helices (Fig. 4*a*)[21,22]. This tertiary interaction is essential for *Azoarcus* activity because it positions the 5'-exon splice site into the intron's active center (J. Strauss-Soukup & S.A.S., unpublished results). The sequence within the P8 tetraloop receptor is identical to the J6a/6b receptor except that the base pair under the G·U wobble is a C–G rather than an U–A pair (Fig. 1*a*). We used an L-9 G206 form of the *Azoarcus* intron which binds to the oligoribonucleotide substrate CAUAAA and ligates the As from the substrate onto the 3'-end of the intron in a reaction analogous to the reverse of the second step of splicing[23]. By performing the reaction with a 3'-end labeled substrate, the active molecules in the population become radioactively tagged[15]. Using this selection strategy we observed $S^6G\alpha S$ interference at two sites: G151, which is equivalent to G227 in the *Tetrahymena* tetraloop receptor, and G92, which is in the major groove three stranded junction between P4 and J6/7 (Fig. 4*b*). We also observed $G\alpha S$ interference at G128, which is in the guanosine binding site[24].

As was true for G227 in the P4-P6 folding assay, interference at G151 was rescued by the addition of 1 mM Tl^+ (Fig. 4*b*). Furthermore, interference at G92 and G128 were not suppressed by Tl^+ addition, consistent with their role in RNA–RNA rather than RNA–metal interactions[24,25]. Because the *Azoarcus* 3'-exon ligation assay is much easier to perform than the P4-P6 folding assay, it was possible to explore the rescue of $S^6G\alpha S$ interference under a wide variety of reaction conditions (Fig. 4*c*). Partial rescue was observed at Tl^+ concentrations as

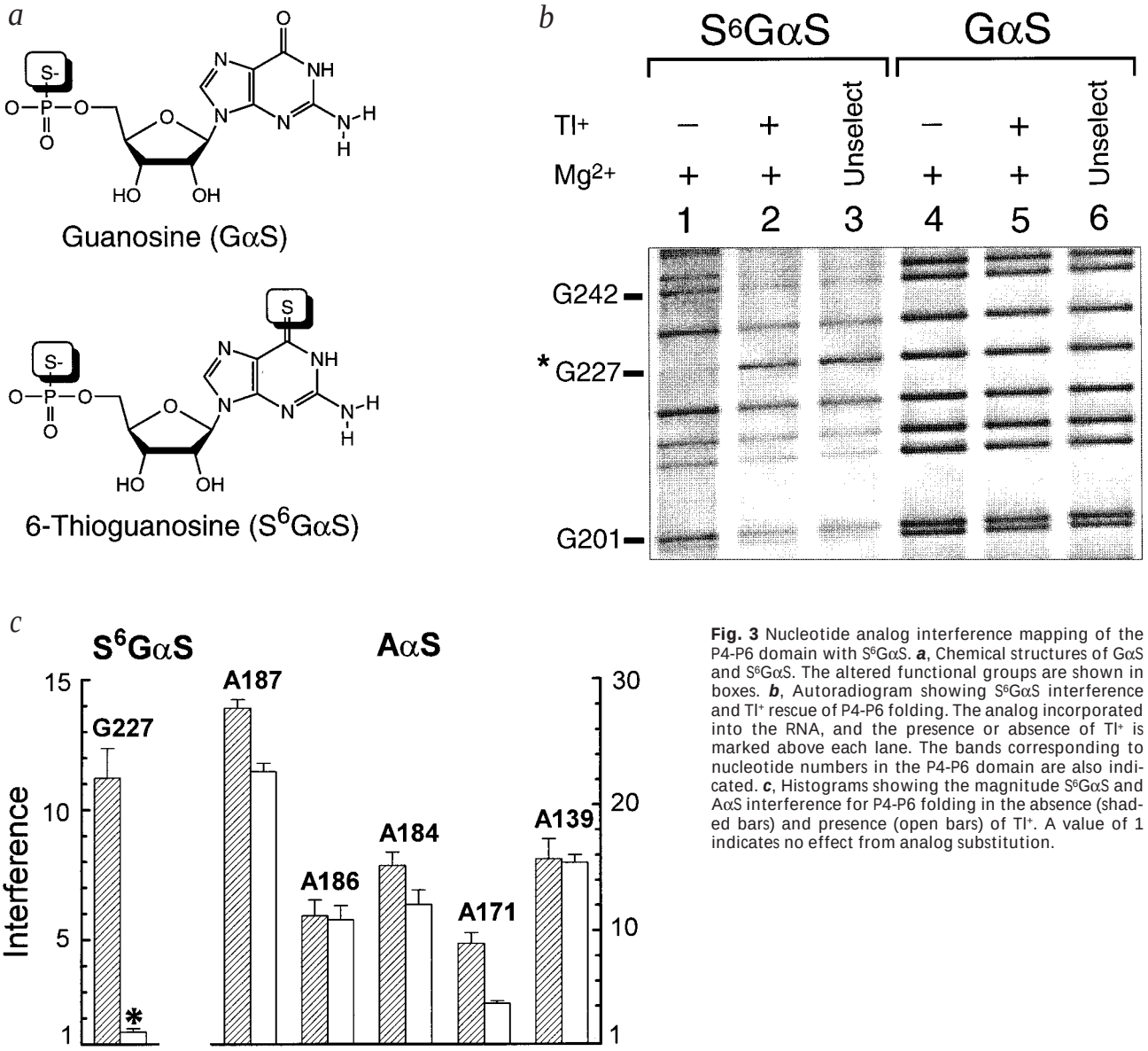

Fig. 3 Nucleotide analog interference mapping of the P4-P6 domain with S^{6}GαS. ***a***, Chemical structures of GαS and S^{6}GαS. The altered functional groups are shown in boxes. ***b***, Autoradiogram showing S^{6}GαS interference and Tl$^+$ rescue of P4-P6 folding. The analog incorporated into the RNA, and the presence or absence of Tl$^+$ is marked above each lane. The bands corresponding to nucleotide numbers in the P4-P6 domain are also indicated. ***c***, Histograms showing the magnitude S^{6}GαS and AαS interference for P4-P6 folding in the absence (shaded bars) and presence (open bars) of Tl$^+$. A value of 1 indicates no effect from analog substitution.

low as 100 μM, and interference was completely rescued at a Tl$^+$ concentration of 750 μM. By contrast, no rescue was observed by addition of up to 100 mM concentrations of the monovalent ions sodium, potassium, rubidium, cesium and ammonium (Fig. 4*c*). Nonspecific interference rescue at G151 and G92 was detected by the addition of very high, non-physiological concentrations of Mg^{2+} (50 mM). Other than the submicromolar Tl$^+$ concentrations, the only specific rescue of G151 interference came from moderately high concentrations (5 mM) of Mn^{2+}, which is a thiophilic divalent ion[26]. However, Mn^{2+} did not rescue as efficiently as Tl$^+$ and a ten-fold higher concentration of Mn^{2+} ion was required to achieve even partial rescue. Given that Mn^{2+} does not bind to the all oxygen form of the AA platform[11], the inefficient Mn^{2+} rescue most likely reflects the creation of an artificial Mn^{2+} binding site due to the S^{6}GαS substitution at G151. These interference data indicate that there is a monovalent metal ion binding site within the tetraloop receptor of the *Azoarcus* group I intron and that metal binding to this site is important for group I intron splicing.

K$^+$ enhances *Azoarcus* activity

The conditions used for P4-P6 crystallization suggest that potassium is the physiologically relevant monovalent metal ion located under the AA platform[6]. Given that a similar monovalent site exists within the *Azoarcus* intron, the inclusion of potassium in the reaction buffer should have a positive effect upon ribozyme activity. To test this possibility, we transcribed the L-9 G206 form of the *Azoarcus* intron without any phosphorothioate substitutions, dialyzed it extensively to remove the metal ions present during transcription, and measured the kinetics of 3'-exon ligation in the presence of several different monovalent metal ions. While there is some activity in the absence of any monovalent ions, the addition of 5 mM K$^+$ increases the k_{cat}/K_m of the ribozyme reaction (Fig. 4*d*). This effect is specific to K$^+$, as the inclusion of 5 mM Na$^+$ slightly decreases k_{cat}/K_m, as does the inclusion of Li$^+$ and Cs$^+$. Other than K$^+$, Tl$^+$ is the only monovalent ion that improves the rate of the reaction, though the effect is very small. The almost six-fold increase in k_{cat}/K_m that is observed between the K$^+$ and Na$^+$ experiments is consistent with

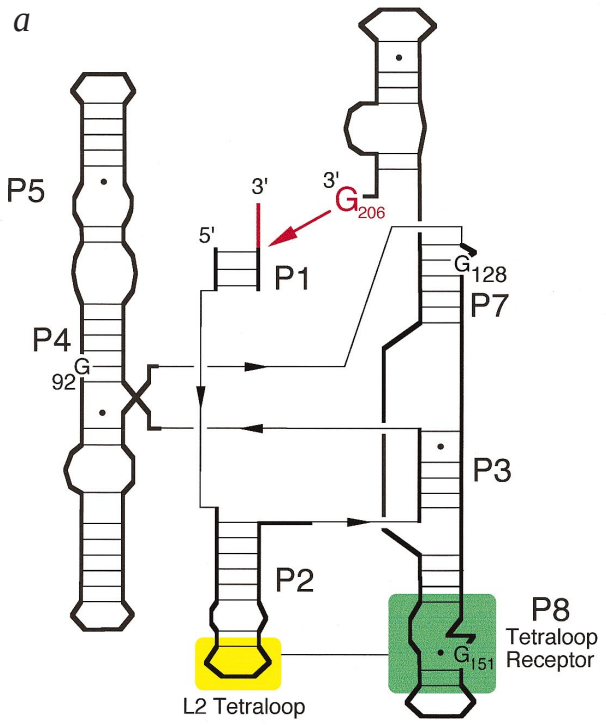

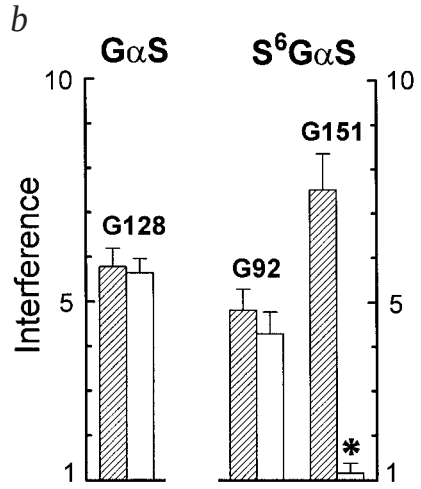

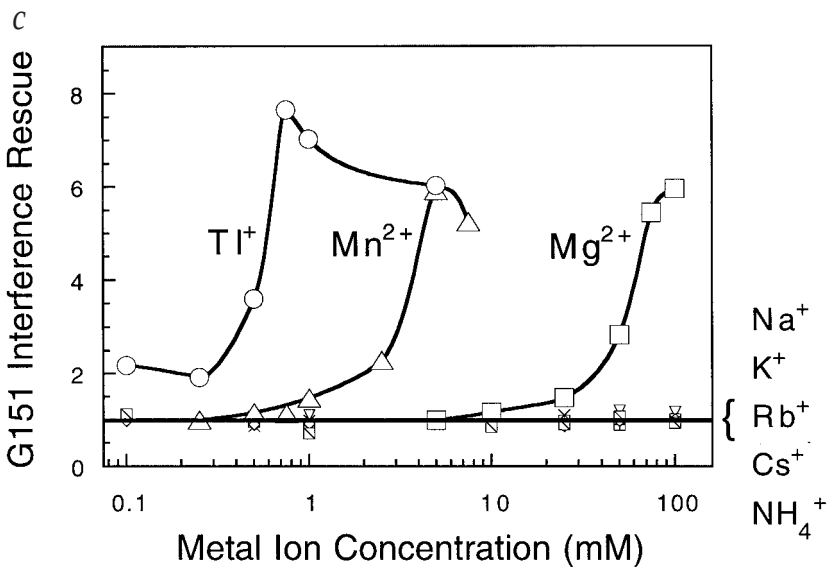

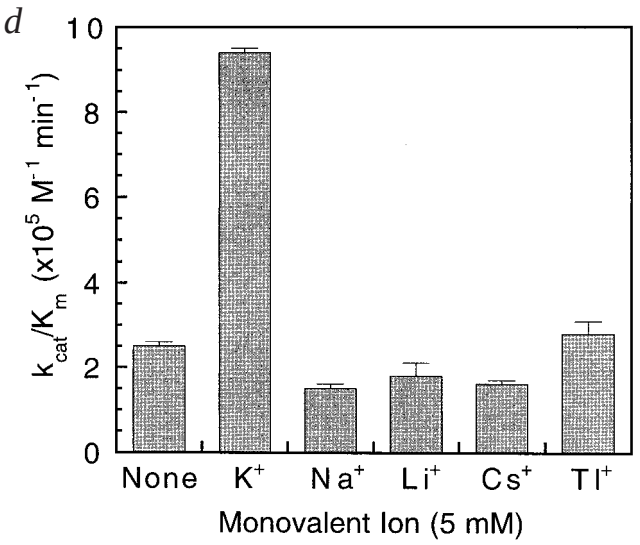

Fig. 4 Interference mapping of the *Azoarcus* group I intron. ***a***, Secondary structure of the L-9 G206 form of the *Azoarcus* intron highlighting the GAAA tetraloop in P2 (yellow) and the tetraloop receptor in P8 (green). This form of the intron performs a 3'-exon ligation reaction that transfers the 3'-end of the oligonucleotide substrate (red) onto the 3'-end of the intron at G206 (red)[15]. ***b***, Histogram showing S^6GαS and GαS interference of the *Azoarcus* group I intron splicing. Interference in the absence of Tl^+ is shown as shaded bars, and interference in the presence of 1 mM Tl^+ is shown as open bars. A value of 1 indicates no effect from analog substitution. ***c***, Plot of S^6GαS interference rescue at G151 as a function of cation concentration. In this plot a value of 1 indicates no rescue was observed, while a value of 8 represents complete rescue. ***d***, Second order rate constants (k_{cat}/K_m) of the *Azoarcus* L-9 G206 ribozyme as a function of the monovalent metal ion indicated below the graph added at a concentration of 5 mM.

the role that the P8 tetraloop receptor plays in docking the P1-P2 substrate helices into the intron active site, and suggests that the physiologically relevant ion in the P8 tetraloop receptor is potassium. Together these data on two distinct group I introns whose tetraloop receptors are located in completely different domains of their respective sequences argue that the potassium ion bound under the AA platform is an integral and conserved element of the tetraloop receptor.

Monovalent ions in RNA folding

While monovalent metal ion binding sites have been identified in many proteins[27–29], there is a limited precedent for specific monovalent metal ion binding sites within RNA. Na^+ ions have been observed in the minor groove of ApU dinucleotide helices[30], and K^+ or Na^+ ions stabilize DNA and RNA G-tetraplexes by stacking between the layers of the G tetrad planes[31,32]. The ions coordinate to the O6 atoms of four or eight different Gs[33]. RNA tetraplexes have been proposed to dimerize the HIV genome during retroviral packaging[34], but no other natural examples of RNA tetraplexes have been reported. The 1.6 Å crystal structure of the pseudoknot from Beet Western Yellow Virus involved in translational frameshifting includes two Na^+ ions that may stabilize the

structure (L. Su, L. Chen, I. Berger, J. Berger, M. Egli & A. Rich, unpublished results). The only other precedent for a specific monovalent ion binding site in RNA is a single potassium or ammonium ion that stabilizes folding of a 58-nucleotide fragment from *E. coli* 23S rRNA[35], though the location of the binding site within the fragment is not known.

From the data presented here and previous studies on P4-P6 folding, we conclude that the P4-P6 domain is stabilized by three different types of metal binding sites. Fully hydrated magnesium ions make outer sphere coordination with the major groove of the RNA helices particularly at consecutive G·U pairs[12]. Several magnesium ions also make inner sphere coordination with specific functional groups (phosphate oxygens and O6 carbonyls of G) located within the metal ion core of the domain[11]. The present work defines a third class of metal ion binding sites, involving potassium ions that make inner sphere coordination to functional groups located immediately under the AA platform.

What distinguishes the potassium ion sites from other divalent sites within RNA? The ionic size, coordination geometry, and free energy of hydration are all likely to affect the specificity of metal ion binding[36]. Magnesium ions are predominantly octahedral in the symmetry of their coordination complexes and have bond distances of 2.2–2.4 Å[37]. Potassium ions have longer bond distances (2.4–2.7 Å) and can adopt irregular coordination geometries and bond angles[33,37]. Furthermore, the free energy of hydration for K^+ and Tl^+ is substantially less than that for Mg^{2+} (80, 82 and 460 kcal mol^{-1} respectively) which could affect the affinity of a metal ion for a specific site. We expect that the larger size, less stringent coordination geometries, and lower hydration energies of Tl^+ and K^+ relative to Mg^{2+} allow these ions to bind beneath the platform.

This work demonstrates that a potassium ion is coordinated directly underneath the AA platform of the tetraloop receptor and that it stabilizes P4-P6 domain folding and enhances *Azoarcus* group I intron splicing. Tl^+ binding can be used in place of K^+ to locate monovalent metal ion binding sites in other RNA crystallographic studies, and S^6GαS interference coupled with Tl^+ rescue provides a convenient biochemical probe to test for such sites in RNAs for which crystals are not available. Tl^+ also provides a biochemical tool for spectroscopic probing of potassium ion binding sites[38,39]. The prevalence of the tetraloop receptor motif and the observation that monovalent ions facilitate the *in vitro* activity of many ribozymes suggest that specific monovalent ion binding sites such as those observed in the P4-P6 domain and the *Azoarcus* group I intron will be present within a variety of RNA structures.

Methods

Monovalent ion soaks into P4-P6 crystals. Crystals were grown as described[40]. Monovalent ions soaks were performed by transferring the crystals to a solution containing 25% methylpentanediol, 75 mM tris-cacodylate pH 6.0, 50 mM magnesium acetate, 0.5 mM spermine, 100 µM cobalt-hexammine, 10% isopropanol and either 25 mM TlOAc or 100 mM CsOH buffered to pH 6.0 with cacodylic acid. Crystals were flash frozen in liquid propane cooled with liquid nitrogen. Anomalous difference maps were calculated from X-ray diffraction data collected by the inverse beam method to 3.5 Å on an R-AXIS II imaging plate area detector and combined with phases from the native experimental density map[8]. The data were processed with DENZO and scaled with SCALEPACK. Electron density maps were produced with CCP4.

Interference mapping of P4-P6 with 6-thioguanosine. The 5'-*O*-(1-thio)-6-thioguanosine triphosphate was synthesized following the general procedures previously described[41]. ^{31}P NMR (H_2O): 43.25 (m), -5.92 (d), -22.74 (t); λ_{max}: 341 nm. The extinction coefficient of S^6G at 341 nm is 21,000 $M^{-1}\cdot cm^{-1}$ at pH 7.5[42].

S^6GαS or GαS were incorporated into the P4-P6 transcript by T7 RNA polymerase in 40 mM Tris-HCl, pH 7.5, 4 mM spermidine, 10 mM DTT, 20 mM $MgCl_2$, 0.05% Triton X-100, and 0.06 mg ml^{-1} DNA template. For S^6GαS transcription 2 mM each of ATP, CTP, UTP and 1 mM GTP were used with 1.25 mM of the analog and 0.4 mM Mn^{2+}. GαS and AαS were incorporated using 2 mM of each NTP and 100 mM of GTPαS or ATPαS respectively. The RNAs containing S^6GαS are extremely unstable, so all experiments were performed as rapidly as possible and all manipulations were completed within two days. The P4-P6 RNAs were purified by PAGE (6% denaturing) and 5'-end labeled as described[11]. Gel shift assays to separate the folded and unfolded variants of P4-P6 were performed by incubating the RNAs in buffer containing 33 mM Tris-base, 66 mM HEPES, pH 7.5, 2 mM $Mg(OAc)_2$, and 10% glycerol at 70° C for 10 min, followed by slow cooling to room temperature. The folded RNAs were separated from the unfolded variants by 8% non-denaturing PAGE in 33 mM Tris, 66 mM HEPES, pH 7.5, 0.1 mM EDTA and 2 mM $Mg(OAc)_2$ at 4–6 °C. The Tl^+ rescue experiments were performed by adding 1 mM TlOAc to the incubation and gel matrix buffers. The folded RNA bands were cut from the gel and eluted into TE overnight. Full-length RNAs were repurified by 8% denaturing PAGE, cut from the gel, eluted into TE containing 2% SDS for 2 h at 4 °C, phenol/chloroform extracted, and ethanol precipitated. The RNAs were redissolved in TE and the phosphorothioate linkages cleaved by the addition of one-tenth volume of 50 mM iodine in ethanol and the cleavage products resolved by 8% denaturing PAGE. The magnitude of the interference was quantitated on a Molecular Dynamics Storm 860 as previously described[20].

Interference mapping of the Azoarcus intron with 6-thioguanosine. S^6GαS and GαS were incorporated into the L-9 G206 form of the *Azoarcus* RNA by T7 RNA polymerase as described for P4-P6. The oligoribonucleotide substrate (CAUAAA) was 3' end labeled with yeast poly(A)polymerase and [α-^{32}P]cordycepin[43]. The radiolabeled substrate was purified by non-denaturing 20% PAGE and eluted from the gel in water. The ligation reactions were performed by preincubating the *Azoarcus* L-9 G206 RNA (250 nM) at 50 °C for 8 min in reaction buffer containing 33 mM Tris-base, 66 mM HEPES pH 7.5, 3 mM $Mg(OAc)_2$, 1 mM $Mn(OAc)_2$ and the additional cations shown in Fig. 4*c*. The samples were cooled to 30 °C, the radiolabeled substrate (10 nM) was added, and the reaction allowed to proceed for 5 min before it was quenched with two volumes of 40% formamide in TE. The reactions were split into two portions, one was treated with one-tenth volume of 50 mM iodine in ethanol, and the cleavage products were separated by 8% denaturing PAGE. In parallel with the ligation assay, the distribution of S^6GαS and GαS incorporation within the L-9 G206 RNAs were determined by 5'-end labeling the RNA, treating with iodine and resolving the cleavage products by 8% PAGE. The band intensities of the ligated and 5'-end labeled control RNAs were used to quantitate the magnitude of interference at each position in the RNA as previously described[20].

Kinetic measurements of *Azoarcus* splicing. The L-9 G206 form of the *Azoarcus* intron was transcribed as reported above except phosphorothioate tagged nucleotides were omitted from the reaction. The RNA was gel purified, eluted into 25 mM TE pH 8.0, ethanol precipitated, and dialyzed against 50 mM tris-HCl pH 7.5 for three days at 4 °C. The buffer was changed every 12 h. The splicing reactions were performed at variable concentrations of the L-9 G206 ribozyme (10 nM to 3 µM) in 100 µM $MgCl_2$, 100 µM spermidine, 25 mM Tris-MES pH 6.0 and 5 mM of various monovalent metal ions using a trace amount of the oligonucleotide substrate CAUAAA radiolabeled at its 3'-terminus. A portion of the reaction was removed at several time points and formamide loading buffer added to stop the reaction. The ligated and unligated substrates were separated by PAGE. The rate constant (k_{obs}) at each ribozyme concentration was calculated by plotting fraction ligated versus time and fitting to a exponential decay with an endpoint of 12%. A plot of k_{obs} versus enzyme concentration was used to calculate k_{cat}/K_m for each reaction condition.

Acknowledgments

We wish to thank P. B. Moore and J. R. Williamson for critical comments on the manuscript. R.P.R. and J.H.C. were supported by the NIH and A.R.F is a Fellow of the Jane Coffin Childs Memorial Fund for Medical Research. J. S.-S. is a Fellow of the NIH. S.A.S. and J.A.D. are both supported by Beckman Young Investigator Awards and the Searle Foundation. J.A.D. is a Lucille P. Markey Scholar and a David and Lucile Packard Foundation Fellow. This work was funded by an NSF CAREER award and a JFRA from the ACS to S.A.S., and by an NIH grant to J.A.D.

Received 24 July, 1998; accepted 14 September, 1998.

1. Pyle, A.M. Ribozymes: a distinct class of metalloenzymes. *Science* **261**, 709–714 (1993).
2. Pyle, A.M. Catalytic reaction mechanisms and structural features of group II intron ribozymes. in *Catalytic RNA*, Vol. 10 (eds Eckstein, F. & Lilley, D.M.J.) 75–107 (Springer, New York; 1996).
3. Nolan, J.M. & Pace, N.R. Structural analysis of the bacterial ribonuclease P RNA. in *Catalytic RNA*, Vol. 10 (eds. Eckstein, F. & Lilley, D.M.J.) 109–128 (Springer, New York; 1996).
4. Miskin, R., Zamir, A. & Elson, D. Inactivation and reactivation of ribosomal subunits: the peptidyl transferase activity of the 50S subunit of *Escherichia coli*. *J. Mol. Biol.* **54**, 355–378 (1970).
5. Zamir, A., Miskin, R. & Elson, D. Inactivation and reactivation of ribosomal subunits: amino acyl-transfer RNA binding activity of the 30S subunit of Escherichia coli. *J. Mol. Biol.* **60**, 347–364 (1971).
6. Manning, G.S. The molecular theory of polyelectrolyte solutions with applications to the electrostatic properties of polynucleotides. *Quart. Rev. Biophys.* **2**, 179–246 (1978).
7. Costa, M. & Michel, F. Frequent use of the same tertiary motif by self-folding RNAs. *EMBO J.* **14**, 1276–1285 (1995).
8. Cate, J.H. *et al.* Crystal structure of a group I ribozyme domain: principles of RNA packing. *Science* **273**, 1678–1685 (1996).
9. Cate, J.H. *et al.* RNA tertiary structure mediation by adenosine platforms. *Science* **273**, 1696–1699 (1996).
10. Murphy, F.L. & Cech, T.R. GAAA tetraloop and conserved bulge stabilize tertiary structure of a group I intron domain. *J. Mol. Biol.* **236**, 49–63 (1994).
11. Cate, J.H., Hanna, R.L. & Doudna, J.A. A magnesium ion core at the heart of a ribozyme domain. *Nature Struct. Biol.* **4**, 553–558 (1997).
12. Cate, J.H. & Doudna, J.A. Metal-binding sites in the major groove of a large ribozyme domain. *Structure* **4**, 1221–1229 (1996).
13. Pauling, L. *The Nature of the Chemical Bond*, (Cornell University Press, Ithaca, NY, 1960).
14. Gaur, R.K. & Krupp, G. Modification interference approach to detect ribose moieties important for the optimal activity of a ribozyme. *Nucleic Acids Res.* **21**, 21–26 (1993).
15. Strobel, S.A. & Shetty, K. Defining the chemical groups essential for *Tetrahymena* group I intron function by nucleotide analog interference mapping. *Proc. Natl. Acad. Sci. USA* **94**, 2903–2908 (1997).
16. Pearson, R.G. Acids and Bases. *Science* **151**, 172–177 (1966).
17. Heitner, H.I., Lippard, S.J. & Sunshine, H.R. Metal binding by thionucleosides. *J. Amer. Chem. Soc.* **94**, 8936–8937 (1972).
18. Gish, G. & Eckstein, F. DNA and RNA sequence determination based on phosphorothioate chemistry. *Science* **240**, 1520–1522 (1988).
19. Boeyens, J.C.A. & Herbstein, F.H. Ionic complexes of thiourea. II. Chemical and crystallographic survey and determination of the crystal structures of some representative complexes. *Inorg. Chem.* **6**, 1408–1425 (1967).
20. Ortoleva-Donnelly, L., Szewczak, A.A., Gutell, R.R. & Strobel, S.A. The chemical basis of adenosine conservation throughout the *Tetrahymena* ribozyme. *RNA* **4**, 498–519 (1998).
21. Reinhold-Hurek, B. & Shub, D.A. Self-splicing introns in tRNA genes of widely divergent bacteria. *Nature* **357**, 173–176 (1992).
22. Tanner, M.A. & Cech, T.R. Activity and thermostability of the small self-splicing group I intron in the pre-tRNA^{Ile} of the purple bacterium *Azoarcus*. *RNA* **2**, 74–83 (1996).
23. Beaudry, A.A. & Joyce, G.F. Directed evolution of an RNA enzyme. *Science* **257**, 635–641 (1992).
24. Michel, F., Hanna, M., Green, R., Bartel, D.P. & Szostak, J.W. The guanosine binding site of the *Tetrahymena* ribozyme. *Nature* **342**, 391–395 (1989).
25. Michel, F., Ellington, A.D., Couture, S. & Szostak, J.W. Phylogenetic and genetic evidence for base-triples in the catalytic domain of group I introns. *Nature* **347**, 578–580 (1990).
26. Pecoraro, V.L., Hermes, J.D. & Cleland, W.W. Stability constants of Mg^{2+} and Cd^{2+} complexes of adenine nucleotides and thionucleotides and rate constants for formation and dissociation of MgATP and MgADP. *Biochemistry* **23**, 5262–5271 (1984).
27. Villeret, V., Huang, S., Fromm, H.J. & Lipscomb, W.N. Crystallographic evidence for the action of potassium, thallium, and lithium on fructose-1,6-bisphosphatase. *Proc. Natl. Acad. Sci. USA* **92**, 8916–8920 (1995).
28. Wilbanks, S.M. & McKay, D.B. How potassium affects the activity of the molecular chaperone Hsc70. II. Potassium binds specifically in the ATPase active site. *J. Mol. Biol.* **270**, 2251–2257 (1995).
29. Doyle, D.A. *et al.* The structure of the potassium channel: molecular basis of K+ conduction and selectivity. *Science* **280**, 69–77 (1998).
30. Rosenberg, J.M. *et al.* Double helix at atomic resolution. *Nature* **243**, 150–154 (1973).
31. Williamson, J.R., Raghuraman, M.K. & Cech, T.R. Monovalent cation-induced structure of telomeric DNA: the G-quartet model. *Cell* **59**, 871–880 (1989).
32. Cheong, C. & Moore, P.B. Solution structure of an unusually stable RNA tetraplex containing G- and U-quartet structures. *Biochemistry* **31**, 8406–8414 (1992).
33. Laughlan, G. *et al.* The high resolution crystal structure of a parallel-stranded guanine tetraplex. *Nature* **265**, 520–524 (1994).
34. Sundquist, W.I. & Heaphy, S. Evidence for interstrand quadruplex formation in the dimerization of human immunodeficiency virus 1 genomic RNA. *Proc. Natl. Acad. Sci. USA* **90**, 3393–3397 (1993).
35. Wang, Y.-W., Lu, M. & Draper, D.E. Specific ammonium ion requirement for functional ribosomal RNA tertiary structure. *Biochemistry* **32**, 12279–12282 (1993).
36. Cox, B.G. & Schneider, H. *Coordination and Transport Properties of Macrocyclic Compounds in Solution* (Elsevier Science Publishers, New York; 1992).
37. Brown, I.B. What factors determine cation coordination numbers? *Acta Crystallogr. B* **44**, 545–553 (1988).
38. Hinton, J.F., Turner, G. & Millett, F.S. Thallous ion interaction with gramicidin incorporated in micelles studied by thallium-205 NMR. *Biochemistry* **21**, 651–654 (1982).
39. Hinton, J.F., Whaley, W.L., Shungu, D., Koeppe, R.E. & Millett, F.S. Equilibrium binding constants for the group I metal cations with gramicidin-A determined by competition studies and Tl+-205 nuclear magnetic resonance spectroscopy. *Biophys. J.* **50**, 539–544 (1986).
40. Doudna, J.A., Grosshans, C., Gooding, A. & Kundrot, C.E. Crystallization of ribozymes and small RNA motifs by a sparce matrix approach. *Proc. Natl. Acad. Sci. USA* **90**, 7829 (1993).
41. Arabshahi, A. & Frey, P.A. A simplified procedure for synthesizing nucleoside 1-thiotriphosphates: dATPαS, dGTPαS, UTPαS, and dTTPαS. *Biochem. Biophys. Res. Com.* **204**, 150–155 (1994).
42. Fox, J.J., Wempen, I., Hampton, A. & Doerr, I.L. Thiation of nucleosides. I. Synthesis of 2-amino-6-mercapto-9-β-D-ribofuranosylpurine ("thioguanosine") and related purine nucleosides. *J. Org. Chem.* **80**, 1669–1675 (1957).
43. Lingner, J. & Keller, W. 3'-end labeling of RNA with recombinant yeast poly(A) polymerase. *Nucleic Acids Res.* **21**, 2917–2920 (1993).
44. Carson, M. RIBBONS 2.0 *J. Appl. Crystallogr.* **47**, 110 (1991).